

# POST CRITICAL HEAT TRANSFER AND FUEL CLADDING OXIDATION

VOJTĚCH ČAHA\*, JAKUB KREJČÍ

Department of Nuclear Reactors, Faculty of Nuclear Sciences and Physical Engineering, Czech Technical University in Prague, Czech Republic

\* corresponding author: [vojtech.caha@jfifi.cvut.cz](mailto:vojtech.caha@jfifi.cvut.cz)

**ABSTRACT.** The knowledge of heat transfer coefficient in the post critical heat flux region in nuclear reactor safety is very important. Although the nuclear reactors normally operate at conditions where critical heat flux (CHF) is not reached, accidents where dryout occur are possible. Most serious postulated accidents are a loss of coolant accident or reactivity initiated accident which can lead to CHF or post CHF conditions and possible disruption of core integrity. Moreover, this is also influenced by an oxide layer on the cladding surface. The paper deals with the study of mathematical models and correlations used for heat transfer calculation, especially in post dryout region, and fuel cladding oxidation kinetics of currently operated nuclear reactors. The study is focused on increasing of accuracy and reliability of safety limit calculations (e.g. DNBR or fuel cladding temperature). The paper presents coupled code which was developed for the solution of forced convection flow in heated channel and oxidation of fuel cladding. The code is capable of calculating temperature distribution in the coolant, cladding and fuel and also the thickness of an oxide layer.

**KEYWORDS:** heat transfer, post dryout, cladding oxidation, isolated channel.

## 1. INTRODUCTION

The post critical heat flux heat transfer is encountered when the surface temperature becomes too high to maintain a continuous liquid contact, and the surface becomes covered by a continuous vapour blanket. It results in coverage of the heated surface by a continuous vapour film in the case of film boiling regime, or an intermittent vapour film in the case of transition boiling regime. The boundary between these post dryout heat transfer boiling regimes is the minimum of film boiling temperature, or Leidenfrost temperature. The typical boiling curve is depicted in Figure 1. Post dryout heat transfer is initiated as soon as the critical heat flux condition is reached and it remains until rewetting or quenching of the surface takes place.

The post critical heat flux heat transfer regimes in boiling flow can be divided as:

- (1.) transition boiling regime,
- (2.) flow film boiling regime,
  - (a) inverted annular film boiling,
  - (b) slug flow film boiling,
  - (c) dispersed flow film boiling.

The transition boiling is a combination of unstable film boiling and unstable nucleate boiling consecutively existing at a given location on a heating surface. Whereas, film boiling is generally defined as a boiling where only the vapour phase is in contact with the heated surface. Inverted annular film boiling is characterized by a vapour layer separating the continuous liquid core from the heated surface and usually encountered at void fractions below 40%. While dispersed flow film boiling is characterized by the existence of

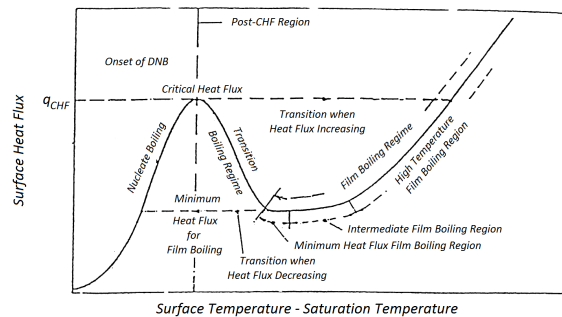


FIGURE 1. Typical boiling curve [1].

discrete liquid drops entrained in a continuous vapour flow; normally encountered at void fractions above 80%. The transition between these two cases is the slug flow film boiling.

The existence of film boiling depends on flow conditions and surface temperature. The main parameters influenced heat transfer in post dryout region are pressure, equilibrium quality and mass flux. Severe non-equilibrium conditions between liquid and vapour phase can occur and must be taken into account in calculation during low coolant mass flux.

It is important to point out that post dryout transition behaviour is reliant on independent boundary condition. If heat flux is the independent boundary condition, the transition boiling regime does not occur. In contrary, when wall temperature is an independent variable, each post dryout flow regime can succeed. As a consequence, the nucleate boiling regime is immediately followed by film boiling regime in the nuclear reactor core [1].

## 2. BASIC EQUATIONS

First, the main objective of the project was to develop a program for the thermo-hydraulic calculation of nuclear reactor core or experimental electrically heated tubes and rod bundles cooled by light water. The temperature profile of the fuel cladding and fuel with the influence of oxide layer was also included. Eventually, the program was used for a comparative assessment of different heat transfer coefficient correlations in the post dryout region and also for evaluation of fuel cladding oxidation correlations.

As a conservative approach for the solution of this calculation is used a method of isolated channel model. The calculation can be conducted for stationary states as well as for transients (pseudo-stationary model). It is possible to input nonuniform power distribution and also local resistance (spacer and mixing grids). The program considers homogeneous equilibrium model (HEM) which respects thermodynamic imbalance between phases. The calculation can be run at constant pressure or with respect to pressure drops. There are included pressure drops caused by friction, spacer and mixing grids, change of elevation and change of coolant density. Pressure drops related to friction between coolant and wall are determined by Fiolenko correlation [2]. The wall temperature correction is set by Protopov correlation [2] and two phase region correction is calculated by Armand's model [2]. The calculation is based on the solution of equation

$$h = \int_0^L Q(z) dz. \quad (1)$$

The thermo-physical properties of light water are evaluated by a library using IAPWS-IF97 definition. The program also contains equations and correlations for real quality, slip ratio, void fraction etc.

During the development, the code was aimed to a simplicity of input data entering and an ability of easy addition of new models and correlations.

## 3. HEAT TRANSFER

The fuel cladding surface temperature is very important parameter in operation and safety of nuclear reactors. That is influenced by a local boiling regime and by a suitable correlation for heat transfer from wall to the coolant. In the subcooled liquid region the calculation of Nusselt number is conducted by Dittus-Boelter equation [2]

$$Nu = 0.023 Re^{0.8} Pr^{0.4}. \quad (2)$$

Whereas nucleate boiling occurs when wall temperature exceeds coolant saturation temperature by Jens-Lottes difference [2]

$$\Delta T_{JL} = 0.791 \exp\left(-\frac{p}{6.201 \times 10^6}\right) q^{0.25}. \quad (3)$$

The beginning of bulk boiling is defined by saturation temperature of coolant and then Thom correlation is

used [2]

$$T_w = T_{\text{sat}} + 22.52 \frac{\sqrt{q}}{\exp\left(\frac{p}{8.6875}\right)}. \quad (4)$$

The wall temperature in the transitional region is linearly approximated. The post critical heat flux heat transfer correlation is used immediately after DNBR decreases below one. The user can choose PG-T [3] or Bezrukov [2] critical heat flux correlation. Eventually, if equilibrium quality is greater or equal one, convection to superheated steam region is set – Sieder-Tate correlation

$$Nu = 0.021 Re^{0.8} Pr^{0.4} \left(\frac{Pr}{Pr_w}\right)^{0.25}. \quad (5)$$

### 3.1. POST CRITICAL HEAT FLUX HEAT TRANSFER

Due to a large number of post critical heat flux heat transfer correlations, it was necessary to carefully select suitable one for use in pressurized light water reactors. The main criterion for selection was validity range of correlation. Finally, it was chosen seven correlations for the post critical heat flux heat transfer.

A list of chosen post CHF heat transfer correlations and their validity ranges are shown in Table 1. It is obvious that all correlations are valid in wide ranges and covered most of operational and emergency states of PWR. Most of them consider thermo-dynamic equilibrium between the phases, i.e. it assumes that the temperature of vapour phase is equal to the temperature of saturation. In general, these correlations have similar form to Dittus-Boelter correlation. Correlations which respects thermo-dynamic imbalance between the phases, consider superheated steam which coexists with liquid drops. The difference between them is the heat flux calculation using wall temperature and superheated steam temperature. The typical correlation which consider thermo-dynamic imbalance is Groeneveld-Delorme correlation.

Correlation	p [MPa]	G [kg m <sup>-2</sup> s <sup>-1</sup> ]	x [-]
Bishop	4.08–21.9	700–3140	0.07–1
Groeneveld 5.7	0,07–21,5	130–4000	–0,12–3,09
Groeneveld 5.9	3,4–21,5	700–5300	0,1–0,9
Miropolskiy	3,9–21,6	800–4550	0,06–1
Groe.-Delorme	0,7–21,5	130–5200	–0,12–3,09
Condie-Beng.	0,42–21,5	16,5–5234	–0,2–1,73
PDO tables	0,1–20,0	0–7000	–0,2–2,0

TABLE 1. Validity range of used post CHF correlations.

The first correlation considering thermo-dynamic equilibrium is Bishop correlation (6), [1]. The calculation of heat transfer coefficient is applied to the temperature of vapour blanket on the heated surface which can be obtained as the average of wall and

saturation temperature. This correlation is used for example in VIPRE or FRAPTRAN codes.

$$Nu = \frac{0.0193 Re_{vf}^{0.8} Pr_{vf}^{1.23} \left(\frac{q_v}{q_l}\right)^{0.068}}{\left(x + \frac{q_v}{q_l}(1-x)\right)^{-0.68}} \quad (6)$$

The next usually used equation is Groeneveld correlation (7), [4]. The user can find two versions (5.7 and 5.9) in the program. The versions differ in coefficients and validity ranges. This correlation is used in COBRA-FLX and FRAPTRAN codes. The temperature of vapour and liquid are related to the saturation temperature.

$$Nu = \frac{c_1 \left(\frac{Gx d_h}{\alpha \lambda_v}\right)^A Pr_w^B}{\left(1 - 0.1 \left(\left(\frac{q_l}{q_v} - 1\right)(1-x)\right)^{0.4}\right)^{-C}} \quad (7)$$

The program also contains Miropolskiy correlation (8), [5]. It is also correlation which respects thermodynamic equilibrium between the phases. But it is valid only for  $0.23 \leq q \leq 1.16 \text{ MW/m}^2$  and  $8 \leq d_h \leq 24 \text{ mm}$ .

$$Nu = \frac{0.023 \left(\frac{G d_h}{\lambda_v}\right)^{0.8} Pr_w^{0.8} \left(x + \frac{q_v}{q_l}(1-x)\right)^{0.8}}{\left(1 - 0.1 \left(\left(\frac{q_l}{q_v} - 1\right)(1-x)\right)^{0.4}\right)^{-1}} \quad (8)$$

Groeneveld-Delorme correlation (9), [6] is a typical example of correlation which considers thermodynamic imbalance. It is used for example in FRAPTRAN code.

$$Nu = \frac{0.008348 Pr_{vf}^{0.6112}}{\left(\frac{G d_h}{\mu_{vf}} \left(x_a + \frac{q_v}{q_l}(1-x_a)\right)\right)^{-0.8774}} \quad (9)$$

The last correlation which was used in the program is Condie-Bengston correlation (10), [6]. It is an empiric correlation that respects thermo-dynamic equilibrium between the phases.

$$\alpha' = \frac{5.345 \times 10^{-5} Pr_w^{2.2598} Re_v^{(0.6249+0.2043 \ln(x+1))}}{(10^3 \lambda_v)^{-0.4593} d_h^{0.8095} (x+1)^{2.0514}} \quad (10)$$

Moreover, Groeneveld's look-up post dryout tables [7] are included in the program. Its advantage is in the wide range of validity due to the large experimental database which is used and simply searching of heat transfer according to pressure, mass flux equilibrium quality and wall and saturation temperature difference. Besides, basic table model includes corrections for hydraulic diameter, cold wall, narrow gap or local resistances. These tables are used for example in ASSERT-PV code.

#### 4. TEMPERATURE PROFILE AND CLADDING OXIDATION

The module solving fuel temperature profile and cladding oxidation is also included. First, the coolant

and wall temperature calculation is performed. An increase of cladding oxide layer and its influence on cladding temperature calculation is followed. Then, a conduction in the cladding is solved. Heat transfer in fuel-cladding gap calculation is the next step. Finally, the temperature profile in fuel is found. All used models consider a cylindrical geometry.

The temperature increase caused by lower thermal conductivity of  $ZrO_2$  compared to cladding depends on oxide thickness and its thermal conductivity (function of temperature)

$$\Delta T_{ox} = \frac{q d_{ox}}{\lambda_{ox}} \quad (11)$$

The growth of the oxide layer greatly depends on the temperature, cladding material and chemical composition of coolant. The current version of the program contains correlation for low temperature oxidation [8] from MATPRO library, but is prepared for addition another formulae

$$\Delta d_{ox} = 0.175 \exp\left(-\frac{14080}{T}\right)t \quad (12)$$

Heat conduction in the cladding is provided with standard equation of Fourier's law in cylindrical geometry.

The calculation of the heat transfer coefficient in fuel-cladding gap is the most complicated part in the temperature profile determination. State of gap depends on many parameters. The program solves it as a sum of three parts – heat conduction in gas, in fuel-cladding contact and thermal radiation. All parts contain several models and many constants. A detailed description can be found in [9].

The Fourier's law is used also for calculation of temperature profile in the fuel [9]. The heat source is considered radially uniform. Thermal conductivity in fuel respects dependency on temperature, porosity, burnup, cracking, composition etc.

#### 5. POST CHF EXPERIMENTS

There were carried out a whole range of experiments in post dryout region in tubes as well as in rod bundles which most of them are unavailable due to their commercial utilization. Available experiments were carried out at different input parameters (pressure, mass flux, power) and geometries. A comprehensive research was done in [1].

A comparative analysis of post dryout heat transfer coefficient correlations described in Section 3.1 were performed. Owing to wide range of experimental parameters were chosen experiments measured at The Royal Institute of Technology in Stockholm [3]. In these experiments which were carried out over 500 were gained more than 15000 points in post CHF region. The experimental equipment was connected to light water loop and was in the shape of a vertical round tube that was electrically heated. There were

also placed 49 thermocouples on the outer wall at different elevation. The axial power distribution was uniform. Ranges of experimental parameters are given in Table 2.

Heated length [m]	7.0
Inner diameter [m]	0.0100, 0.0149, 0.0247
Inlet coolant subc. [°C]	5 ± 1, 10 ± 3
Pressure [MPa]	3, 5, 7, 10, 12, 14, 16, 18, 20
Mass flux [kg m <sup>-2</sup> s <sup>-1</sup> ]	500, 1000, 1500, 2000, 2500, 3000
Heat flux [MW m <sup>-2</sup> ]	0.10–1.25
Quality (PDO) [-]	0.03–1.60

TABLE 2. Range of experimental parameters and geometry.

## 6. POST CHF EXPERIMENTS RESULTS

The comparison of all described post CHF heat transfer coefficient correlation was performed on the group of 120 experiments which were chosen carefully to satisfy validity ranges of all correlations (Table 1). The calculation found wall temperatures which were compared with experimentally obtained values in the post CHF region. An example of one experiment results is given in Figure 2. The figure shows a dependence of wall temperature on the axial length. Immediately after CHF conditions are reached the rapid increase in wall temperature is observed. Then, the wall temperatures differ due to used correlation.

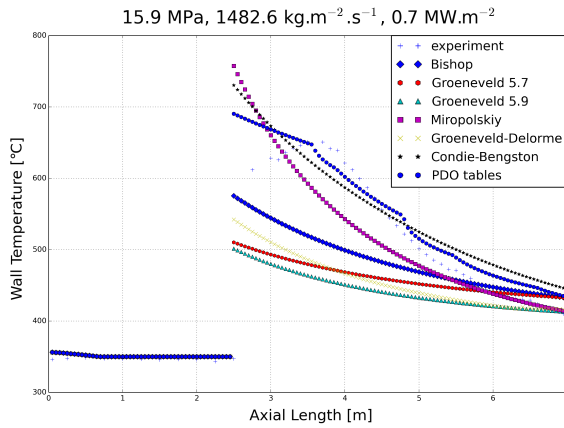


FIGURE 2. Dependence of calculated and experimental wall temperature on axial length.

Another capability of developed program is shown in Figure 3. The graphical module is able to draw any important calculated parameter in time (transient calculations) and also temperature profiles of coolant, cladding and fuel in each time step.

The best results were obtained with Groeneveld's look-up PDO tables. Statistical evaluation is given in Table 3 where

$$\Delta_i = \frac{T_{w,calc,i} - T_{w,exp,i}}{T_{w,exp,i}}, \quad (13)$$

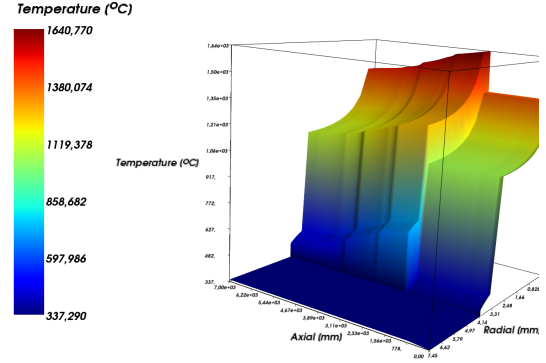


FIGURE 3. Coolant, cladding and fuel temperature profile.

$$\bar{\Delta} = \frac{1}{N} \sum_{i=1}^N \Delta_i, \quad (14)$$

$$\bar{\sigma} = \sqrt{\frac{1}{N-1} \sum_{i=1}^N (\Delta_i - \bar{\Delta})^2}. \quad (15)$$

Correlation	$\bar{\Delta}$ [%]	$\bar{\sigma}$ [%]
Bishop	2.22	8.69
Groeneveld 5.7	0.19	8.3
Groeneveld 5.9	-4.93	7.37
Miropolskiy	12.58	22.37
Groe.-Delorme	92.01	12.08
Condie-Beng.	13.73	13.69
PDO tables	2.82	5.67

TABLE 3. Statistical evaluation of post CHF correlations.

Figure 4 shows a comparison of experimental and calculated wall temperatures achieved with Groeneveld's look-up PDO tables.

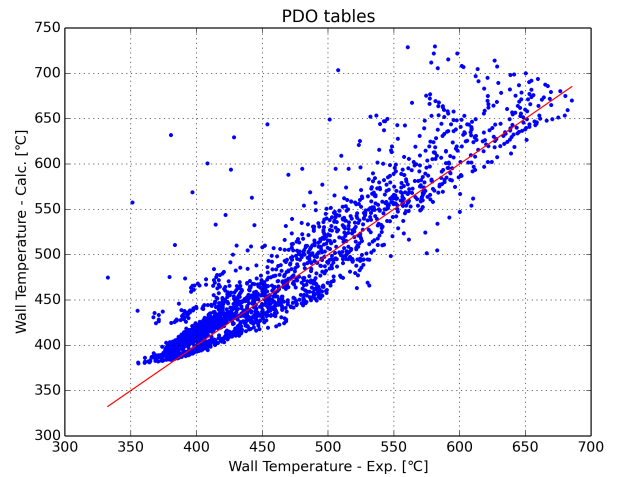


FIGURE 4. Groeneveld's look-up PDO tables results.

## 7. CONCLUSION

A thermo-hydraulic program based on isolated channel model was developed. It includes the wide range of heat transfer correlations for different one phase and two phase flow regimes. Great attention was paid to the post CHF boiling regime. The program also includes the module for evaluation of temperature profile in fuel and cladding which contains influence of oxide layer. The program is prepared for the addition of new oxidation model correlations which are being developed for different cladding tubes materials and temperature ranges. All calculated results can be shown in 3D graphs created by post-processing module using python Mayavi library.

A comparative analysis of different heat transfer correlations in the post CHF region was done. The analysis included a comparison of seven post CHF heat transfer correlations with experimental data which were obtained on electrically heated tube. The best results were achieved with Groeneveld's look-up PDO tables.

The continue of this work should aim to verify this results on different experimental data set with axially nonuniform power distribution, on transient experiment with the return from post CHF region and on rod bundle experiment.

### LIST OF SYMBOLS

$G$	Mass flux [kg/m <sup>2</sup> s]
$h$	Enthalpy [K/kg]
$L$	Length [m]
$q$	Heat flux [W/m <sup>2</sup> ]
$Q$	Linear power [W/m]
$Nu$	Nusselt number [-]
$p$	Pressure [Pa]
$Pr$	Prandtl number [-]
$Re$	Reynolds number [-]
$t$	Time [s]
$T$	Temperature [K]
$x$	Quality [-]
$\alpha$	Void fraction [-]
$\lambda$	Heat transfer coefficient [W/m <sup>2</sup> K]
$\mu$	Dynamic viscosity [Pa s]
$\rho$	Density [kg/m <sup>3</sup> ]

## ACKNOWLEDGEMENTS

This work was supported by the Grant Agency of the Czech Technical University in Prague, grant No. SGS14/156/OHK4/2T/14.

## REFERENCES

- [1] Thermohydraulic relationships for advanced water cooled reactors. Tech. Rep. IAEA-TECDOC-1203, International Atomic Energy Agency, 2001. [http://www.iaea.org/inis/collection/NCLCollectionStore/\\_Public/32/024/32024154.pdf](http://www.iaea.org/inis/collection/NCLCollectionStore/_Public/32/024/32024154.pdf).
- [2] N. E. Todreas, M. Kazimi. *Nuclear Systems Volume I: Thermal Hydraulic Fundamentals*. CRC Press, 1989.
- [3] K. M. Becker, C. H. Ling, S. Hedberg, G. Strand. An experimental investigation of post dryout heat transfer. Tech. Rep. KTH-NEL-33, Royal Institute of Technology, Stockholm, Sweden, 1983. [http://www.iaea.org/inis/collection/NCLCollectionStore/\\_Public/15/049/15049472.pdf](http://www.iaea.org/inis/collection/NCLCollectionStore/_Public/15/049/15049472.pdf).
- [4] D. C. Groeneveld. Post-dryout heat transfer at reactor operating conditions. In *National Topical Meeting on Water Reactor Safety*. 1973. [http://www.iaea.org/inis/collection/NCLCollectionStore/\\_Public/04/089/4089010.pdf](http://www.iaea.org/inis/collection/NCLCollectionStore/_Public/04/089/4089010.pdf).
- [5] N. Hammouda. *Subcooled Film Boiling in Non-Aqueous Fluids*. Ph.D. thesis, University of Ottawa, 1996. <http://hdl.handle.net/10393/9949>.
- [6] S. K. Moon, S. Y. Chun, S. Cho, et al. An experimental study on post-chf heat transfer for low flow of water in a 3x3 rod bundle. *Nuclear Engineering and Technology* **37**(5):457–468, 2005.
- [7] D. C. Groeneveld. Look-up table for fully developed film-boiling heat-transfer coefficients for light water. University of Ottawa, 2001.
- [8] J. Krejčí, V. Vrtílková, D. Gajdoš, D. Rada. Proposal of new oxidation kinetics for sponge base E110 cladding tubes material. In *TopFuel2015 – Conference Proceedings*, pp. 466–473. 2015. <http://www.euronuclear.org/events/topfuel/topfuel2015/transactions/topfuel2015-transactions-poster.pdf>.
- [9] J. Krejčí, V. Čaha. UBE-PostCHF. Tech. rep., ČVUT, Praha, 2015.